Journal of Hazardous Materials 161 (2009) 416–422

Contents lists available at ScienceDirect

Journal of Hazardous Materials

journal homepage: www.elsevier.com/locate/jhazmat

Preparation, characterization and photocatalytic activities of holmium-doped titanium dioxide nanoparticles

Jian-wen Shi[a,*], Jing-tang Zheng[b], Peng Wu[a]

[a] Institute of Urban Environment, Chinese Academy of Sciences, Xiamen, Fujian, 361012, China
[b] The State Key Laboratory of Heavy Oil, China University of Petroleum, Dongying, Shandong, 257061, China

ARTICLE INFO

Article history:
Received 11 December 2007
Received in revised form 4 March 2008
Accepted 26 March 2008
Available online 1 April 2008

Keywords:
Titanium dioxide
Photocatalysis
Photodegradation
Ions doping

ABSTRACT

Holmium-doped TiO_2 nanoparticles with high photocatalytic activities were prepared by sol–gel method and characterized by X-ray diffraction, transmission electron microscopy, ultraviolet–visible diffuse reflectance spectroscopy, and surface area measurement by nitrogen adsorption in this study. Experimental results indicated holmium doping could increase the surface area of TiO_2 nanoparticles, and inhibit the growth of crystalline size and the anatase-to-rutile phase transformation. The results of photodegrading methyl orange showed holmium doping improved the photocatalytic activity of TiO_2, and the reasons could be attributed to the synergetic effects of large surface areas, small crystallite size, lattice distortion and more charge imbalance of holmium-doped TiO_2. In our experiment, the optimal doped amount was 0.3 mol.% for the maximum photocatalytic degradation ratio when holmium-doped TiO_2 was calcined at 500 °C, and the optimal calcined temperature was 600 °C when the doped amount was 0.5 mol.%.

1. Introduction

TiO_2 photocatalyst has attracted extensive interest in the past decades due to its capability of degrading a wide range of both gaseous and aqueous contaminants [1–4]. It appears to be a promising material for air and water pollution control. However, because of its big forbidden band only ultraviolet with the energy of more than 3.2 eV can stimulate its photocatalytic action. Furthermore, the photocatalytic activity of TiO_2 is limited by fast charge carrier recombination and low interfacial charge-transfer rates of photogenerated carriers. In order to overcome these difficulties, two main modified methods are often adopted to improve its photocatalytic performance. One is extending lightwave absorption range of TiO_2 to visible region [5–8]. The other is suppressing the recombination of excited electrons and positive holes [9].

Doping with transition metal ions has been proven a potential route to improve photocatalytic activity of TiO_2 [10,11]. Rare earth metals having incompletely occupied 4f and empty 5d orbitals are often used as catalyst or promote catalysis [12]. Furthermore, doping with lanthanide ions with 4f electron configurations also could significantly improve the separation rate of photoinduced charge carriers in TiO_2 photocatalysts and greatly enhance the photocatalytic activity of TiO_2 [13]. Some investigated results have shown that the photocatalytic activity of TiO_2 could be improved by some rare earth metals doping [14–17]. Xie and Yuan [14,15] fabricated TiO_2 sol modified with europium and cerium ions by chemical coprecipitation–peptization method, and obtained excellent photocatalytic activity for X-3B degradation under visible light irradiation. Xu et al. [17] prepared a series of rare earth metals ions (La^{3+}, Ce^{3+}, Er^{3+}, Pr^{3+}, Gd^{3+}, Nd^{3+} and Sm^{3+}) doped TiO_2 by sol–gel. The results showed rare earth metals ions doping enhanced the photocatalytic activity of TiO_2. However, there is an example that some rare earth ions doping may bring negative effect on the photocatalytic performance of TiO_2. Xiao et al. [18] synthesized cerium-doped mesoporous TiO_2 nanoparticles with high surface areas and thermal stable anatase wall by hydrothermal process. Experimental results indicated that cerium doping not only increased the surface areas of mesoporous TiO_2 nanoparticles, but also inhibited the mesopores collapse and the anatase-to-rutile phase transformation. Moreover, the un-doped and cerium-doped anatase mesoporous nanoparticles exhibited higher photocatalytic activity than commercial photocatalyst (Degussa, P25), but the maximum photodegradation rate was the un-doped mesoporous TiO_2 nanoparticles. The lower photocatalytic activities of cerium-doped sample might be ascribed to that the doped cerium blocked partially the surface sites available for the photodegradation and absorption of Rhodamine B.

Holmium (III) possesses one of the highest magnetic moments of all rare earth metal ions. As such, it has been used as a magnetic material widely [19]. Furthermore, the surface of holmium

* Corresponding author. Tel.: +86 592 2610132; fax: +86 592 2659290.
E-mail address: shijnwn@163.com (J.-w. Shi).

0304-3894/$ – see front matter © 2008 Elsevier B.V. All rights reserved.
doi:10.1016/j.jhazmat.2008.03.114

oxide, Ho_2O_3, crystallizes in a cubic structure, exposes Lewis acid sites and highly reactive base sites (O^{2-} and/or OH^-) [20]. The OH^- could react with holes and produce surface hydroxyl radical, which is advantage to improve the photocatalytic activity of TiO_2. However, as an important member in rare earth metals, holmium used as a dopant to modify titanium dioxide has never been reported. So the present work aims essentially to obtain an effective photocatalyst by doping TiO_2 with holmium ions.

In this work, the holmium-doped TiO_2 nanoparticles were prepared by sol–gel method. The microstructures, such as the crystal phase, the crystallite size, the surface area and the morphology of the individual particle were measured. The effects of holmium ions doped amount and calcined temperature on photocatalytic activity of TiO_2 were also investigated by photocatalytic degrading methyl orange in water under UV irradiation.

2. Experimental

2.1. Samples preparation

The holmium-doped TiO_2 powder samples were prepared by sol–gel route using tetra-*n*-butyl titanate and rare earth metal salt ($Ho(NO_3)_3{\cdot}6H_2O$). One solution containing 28.32 ml ethanol, 7.2 ml distilled water, 20 ml acetic acid and required $Ho(NO_3)_3{\cdot}6H_2O$ was prepared. And, it was slowly added into the other solution that was prepared by stirring 0.05 mol $Ti(OC_4H_9)_4$ into 30 ml ethanol. It is noted that all reagents used in this experiment are analytical grade. The mixture was hydrolyzed for 60 min under vigorous stirring, and the transparent sol was obtained. Gel was prepared by aging the sol for 6 h at 60 °C. To remove the solvents in the acquired gel, the gel was dried in a vacuum box at 80 °C. After that, it was milled to powder by ceramic mortar. Then, the powder samples were calcined at experimental temperature (i.e. 500, 600, 700, and 800 °C, respectively) for 2 h. At the same time, un-doped TiO_2 powder samples were prepared at the same experimental conditions. The un-doped samples were signed as TY, and the holmium-doped samples were labeled as TH(*X*)*Y*, where *X* and *Y* were referred to the molar percentage concentrations of Ho ions and the calcined temperatures, respectively. For example, if a sample was doped with 0.3 mol.% holmium and calcined at 500 °C, it was marked as TH(0.3)500.

2.2. Characterizations

X-ray diffraction (XRD) spectra of all samples were obtained at room temperature with a Holand X'pert PROMPD diffractometer with Cu $K_{\alpha 1}$ radiation operated at 45 kV and 40 mA. The crystalline size was estimated to the full width at half maximum (FWHM) of the (1 0 1) peak of anatase by applying the scherrer equation as follows:

$$D = \frac{K\lambda}{\beta \cos\theta} \quad (1)$$

where K is a constant (shape factor, about 0.89), λ is the X-ray wavelength, β is the FWHM of the diffraction line, and θ is the diffraction angle. The weight fraction of anatase was calculated using Eq. (2) as follows:

$$X_A(\%) = \frac{100}{1 + (1.265 I_R / I_A)} \quad (2)$$

where X_A is the mass fraction of anatase in the samples, I_A and I_R are the X-ray integrated intensities of (1 0 1) peak of the anatase and (1 1 0) peak of rutile, respectively. The lattice distortion was also estimated from the XRD spectra using the formula as follows:

$$\varepsilon = \frac{\beta}{4tg\theta}$$

where ε is the lattice distortion. The determinations of the relative surface areas of the investigated samples were carried out by the Brunauer–Emmett–Teller (BET) adsorption isotherm method using nitrogen as the adsorbate at 77 K. The morphologies of the investigated samples were examined by transmission electron microscope (TEM, JEM-2012). Ultraviolet–visible diffuse reflectance spectroscopy (DRS) of sample was recorded on UV-3000 spectrophotometer in the range 300–600 nm at room temperature in air, using $BaSO_4$ as reference substance.

2.3. Measurement of photocatalytic activity

The process of photodegradation was carried out in a photo reaction system shown in Fig. 1. The reactive bottle was a 250-ml cylindrical vessel with a water-cooled quartz jacket. In the center of the quartz jacket, a 500 watt high-pressure mercury lamp with major emission at 365 nm was used to offer ultraviolet irradiation. In the bottom of the reactor, a magnetic stirrer was equipped to achieve effective dispersion. Air was bubbled through the reaction solution from the bottom to ensure a constant dissolved oxygen concentration (DOC). To assess the photocatalytic activity of doped TiO_2, un-doped TiO_2 powder was also tested. The additive amount of catalyst powder was 2 g/L. The initial methyl orange concentration was 40 mg/L and the temperature of the reaction solution was

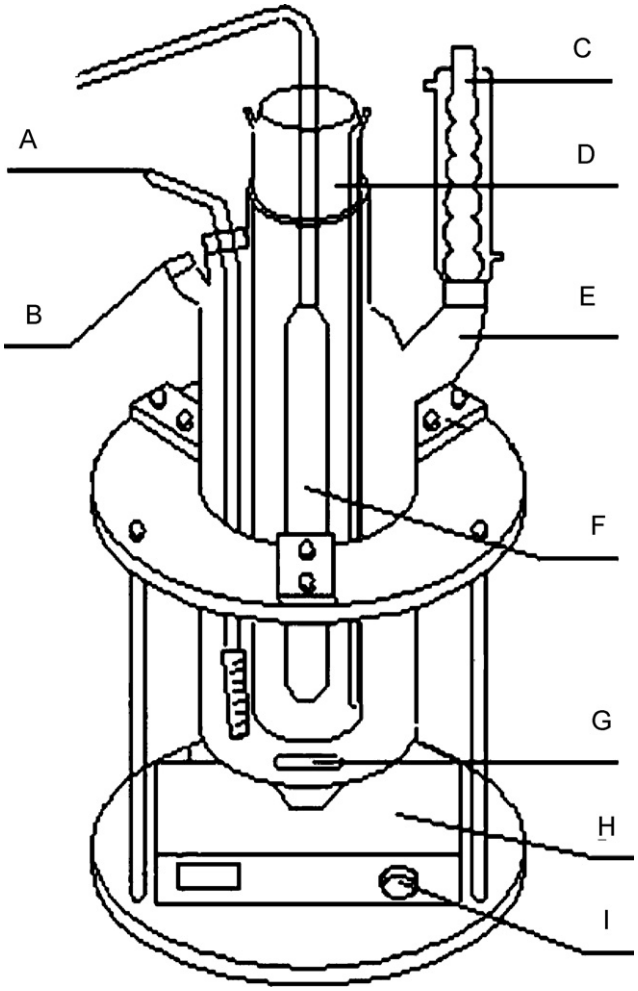

Fig. 1. Photo reaction system: (A) temperature probe; (B) blowhole; (C) condensator; (D) water-cooled quartz jacket; (E) reactive bottle; (F) lamp; (G) magnetic rod; (H) magnetic stirrer; (I) velocity knob.

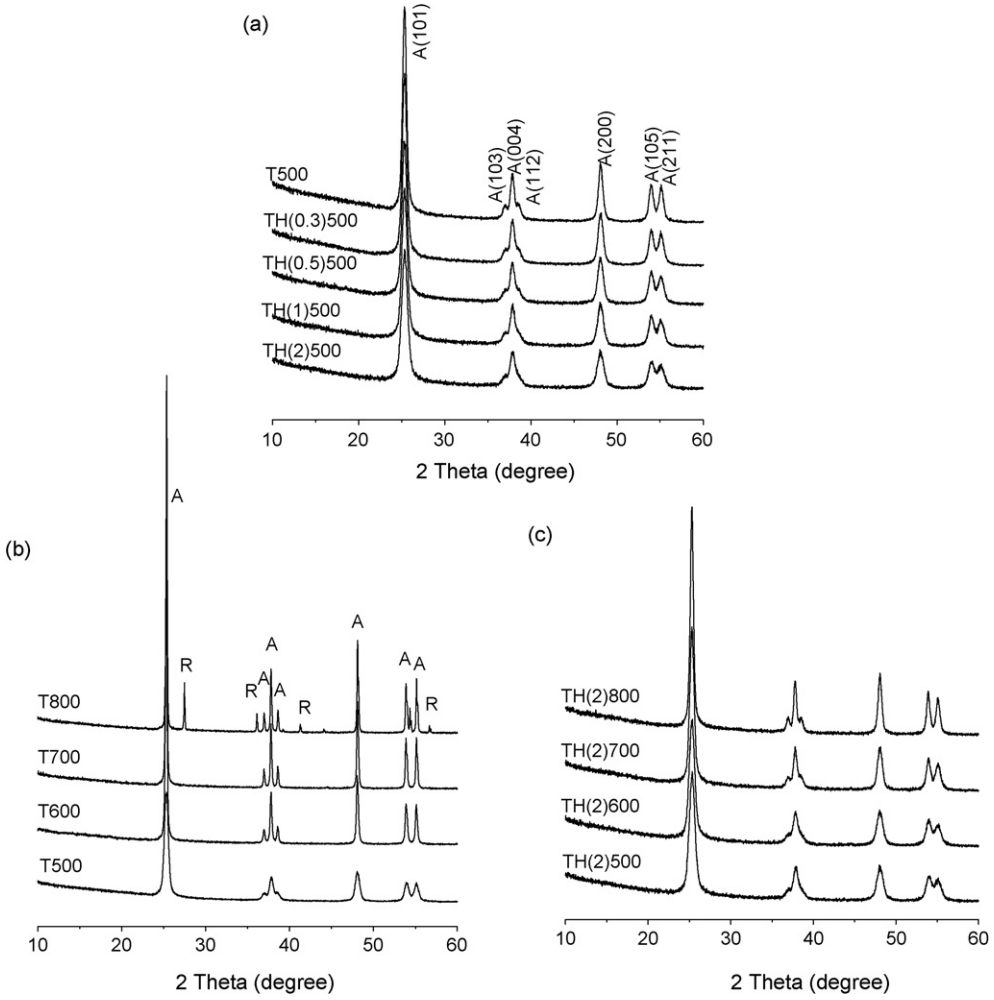

Fig. 2. XRD spectra of samples (A: anatase, R: rutile).

maintained at 30 ± 0.5 °C. Four milliliters samples were withdrawn each 3 min interval. The concentrations of methyl orange in all samples were measured at 465 nm by a spectrophotometer (DR/2500, HACH).

3. Experimental results and discussions

3.1. XRD and BET analyses

The XRD spectra of investigated samples at different experimental conditions (i.e. doped concentrations and calcined temperature) were shown in Fig. 2. It was found that all samples had anatase structure, except for the un-doped TiO_2 sample calcined at 800 °C, which 11 wt.% rutile structure appeared. It indicated that phase transition from anatase-to-rutile was inhibited by holmium ions doping. Lin et al. [21,22] also found that rare earth ions (i.e. Ce^{4+}, La^{3+}, and Y^{3+}) could inhibit the anatase-to-rutile phase transformation during the thermal treatment. The inhibition of the phase transition was ascribed to the stabilization of the anatase phase by the surrounding rare earth ions through the formation of Ti—O rare earth element bonds [23]. In this investigation, it might be ascribed to the formation of Ti—O—Ho interaction.

Along with the increase of holmium-doped amount, the diffraction peaks of anatase phase became broader in width and weaker in intensity (Fig. 2(a)), which implied that holmium doping inhibited the growth of nanocrystallite size. It also was reported that rare earth ions (i.e. Ce^{4+}, Eu^{3+}, and Sm^{3+}) doping inhibited significantly the growth of crystallite size [24,25]. It might be ascribed to that the Ti—O—Ho bonds had formed on the surface of TiO_2 during calcination, which retarded the contact of particles, the transfer and rearrangement of Ti and O in particles [26].

Fig. 2(b) showed the XRD spectra of un-doped TiO_2 calcined at different temperatures. It can be observed that the crystalline development of T500 was uncompleted. The strength of diffraction peaks increased and the outline of diffraction peaks clarified with the increase of calcined temperature. It indicated that high temperature was helpful to improve the crystalline degree.

Fig. 2(c) showed XRD spectra of 2 mol.% holmium-doped samples calcined at different temperatures. No characteristic peak of holmium oxide was found in the XRD patterns. It implied either Ho ions were incorporated in the crystalloid of TiO_2 or holmium oxide was very small and highly dispersed [5].

The characteristics of samples used in this study were summarized in Table 1. Comparing these particles characteristics calcined at 500 °C and doped with different holmium amounts (i.e. 0, 0.3, 0.5, 1.0, and 2.0 mol.%), it was observed that the crystalline size decreased with the increase of doped holmium amount. It also showed that the crystalline size increased with the increase of calcined temperature, and the phenomenon in un-doped TiO_2 was more visible than that in holmium-doped TiO_2, which implied that

Table 1
XRD analyses and BET results of samples

Sample label	Anatase content (%)	Anatase crystalline size (nm)	specific surface area (m^2/g)	Lattice distortion (%)	Crystal parameters		
					a (nm)	c (nm)	V (nm^3)
T500	100	18.2	nd[a]	0.8595	0.3892	0.8084	0.1225
T600	100	51.9	38.42	0.3012	0.3888	0.8166	0.1234
T700	100	79.1	nd[a]	0.1976	0.3898	0.8127	0.1235
T800	89	101.8	0.5873	0.1534	0.3884	0.8221	0.1240
TH(0.3)500	100	15.5	76.76	1.0044	0.3892	0.8119	0.1230
TH(0.5)500	100	15.0	nd[a]	1.0429	0.3898	0.8127	0.1235
TH(1)500	100	14.2	nd[a]	1.1000	0.3889	0.8245	0.1247
TH(2)500	100	12.5	nd[a]	1.2501	0.3887	0.8194	0.1238
TH(2)600	100	13.0	98.81	1.1988	0.3885	0.8252	0.1245
TH(2)700	100	15.1	nd[a]	1.0351	0.3887	0.8251	0.1246
TH(2)800	100	20.5	nd[a]	0.7614	0.3882	0.8286	0.1248

[a] Not determined.

holmium doping inhibited the growth of crystalline size. Smaller crystallite size would contribute to larger surface areas [27]. The surface area increases from 0.5873 m^2/g of T800 to 38.42 m^2/g of T600 is due to the decrease of crystalline size from 101.8 to 51.9 nm. The surface area of TH(2)600 was 98.81 m^2/g, much more than that of T600, it ascribed to the inhibited function of holmium doping. Venkatachalam et al. [28] prepared Zr^{4+} doped nano-TiO_2 and found that the specific surface area shifted towards lower values at higher calcined temperatures and the surface area of the catalysts increased with increase of Zr^{4+} content. They thought this increase was due to Zr^{4+} present on the surface of TiO_2, which inhibited densification and crystalline growth of TiO_2 nanoparticles by providing dissimilar boundaries. Mona Saif et al. [29] investigated Tb-, Eu- and Sm-doped TiO_2 and found that surface area of TiO_2 was remarkably increased because of these lanthanides ions doping, and they also thought that the highest surface area of doped TiO_2 samples was caused by the crystallite size reduction. In Table 1, it can be observed that unit cell volumes and lattice distortion of holmium-doped TiO_2 particles are larger than that of un-doped TiO_2, meaning that a small part of Ti ions was replaced by Ho ions in the TiO_2 lattice, and resulted in the distortion and expansion of crystal lattice. Oxygen molecules were easy to be adsorbed as electron trap on the sites of structure defects brought by the lattice distortion and expansion. So the recombination rate of electron and hole pairs could be reduced, which had a positive influence on the photocatalytic activity of TiO_2 [30].

3.2. TEM analyses

Fig. 3(a and b) displayed the TEM micrographs of holmium-doped and un-doped TiO_2 calcined at 500 °C, respectively. The morphologies of samples presented anomalistic sphericity, and the difference on particle diameter of un-doped TiO_2 was bigger than holmium-doped TiO_2. The average crystalline size of un-doped TiO_2 was also larger than holmium-doped TiO_2, which was approximately consistent with the results of XRD analyses.

3.3. UV–vis diffuse reflectance spectroscopy

Fig. 4 showed the UV–vis diffuse reflectance spectroscopy of un-doped and holmium-doped TiO_2. Comparing with un-doped TiO_2, a tiny blue-shift of the absorption profile and two absorption peaks around at 450 and 540 nm in the holmium-doped TiO_2 were observed in Fig. 4(a). In general, the spectra of rare earth metal (i.e. Gd^{3+}, Nd^{3+}, La^{3+}, Pr^{3+}, Er^{3+}, Ce^{3+}, Sm^{3+}) doped TiO_2 showed red shifts in the band-gap transition [17]. The tiny blue-shift in the present work might be ascribed to quantumsize effective due to the decrease of the crystalline size. In Fig. 4(b), it indicated that the absorption profile shifted slightly to longer wavelengths with the increase of calcined temperature. Red-shift extent of the sample calcined at 800 °C was the biggest among the four samples. It attributed to the appearance of rutile structure confirmed by XRD pattern in Fig. 2(b), whose band-gap energy was smaller than that of anatase structure. The influence of calcined temperature on absorption profile of holmium-doped TiO_2 (Fig. 4(c)) was slight, but the red-shift extent of the sample calcined at 600 °C, not at 800 °C, was the biggest among the four holmium-doped TiO_2 samples, which was different from un-doped TiO_2 samples.

3.4. Photocatalytic activity

The photocatalytic activities of the samples were measured by the degrading aqueous solution of methyl orange without concerning the degradation intermediates in detail. Before degrading with photocatalysts (or a lamp light), the methyl orange solution was stirred under mercury lamp irradiation (or in dark) for half an hour. It showed that the concentration of methyl orange had negligibly changed, which indicated that there was no degradation when photocatalyst (or irradiation) was absent.

The residual concentration ratios (C_t/C_0) of methyl orange versus photocatalytic time under mercury lamp irradiation were shown in Fig. 5. Where, C_0 and C_t (mg/L) were signed as the initial concentration of methyl orange and the concentration at different photocatalytic times (t), respectively. In comparison with un-doped TiO_2, holmium doping improved the photocatalytic activity of TiO_2 markedly. It can be observed from Fig. 5(a) that holmium-doped amount was an important factor affecting photocatalytic activity, and the optimal doped amount was 0.3 mol.% for the maximum photocatalytic degradation ratio. Fig. 5(b and c) showed the photocatalytic activities of un-doped TiO_2 and holmium-doped TiO_2 calcined at different temperatures. The effects of calcined temperature on photocatalytic activities of both un-doped and holmium-doped TiO_2 were very obvious. The optimal and worst calcined temperatures were 600 and 800 °C in the experiments, respectively. Furthermore, the holmium-doped sample revealed its higher catalytic activity. These might be attributed to these differences between un-doped and doped TiO_2, such as crystalline size, specific surface area, catalyst phase, light absorbed property, and so on.

Based on the experimental results above, it can be concluded that holmium doping reduced the crystalline size and increased specific surface area of the investigated samples. Then, the photocatalytic activity of samples was enhanced. The photocatalytic reaction occurred on the surface of the catalysts, and recombination of the photogenerated electron and hole was very fast, so interfacial charge carrier transfer was possible only when the donor or acceptor was pre-adsorbed before the photocatalytic reaction. The preliminary adsorption of the substrates and the amount of adsorption were very important for highly efficient degradation.

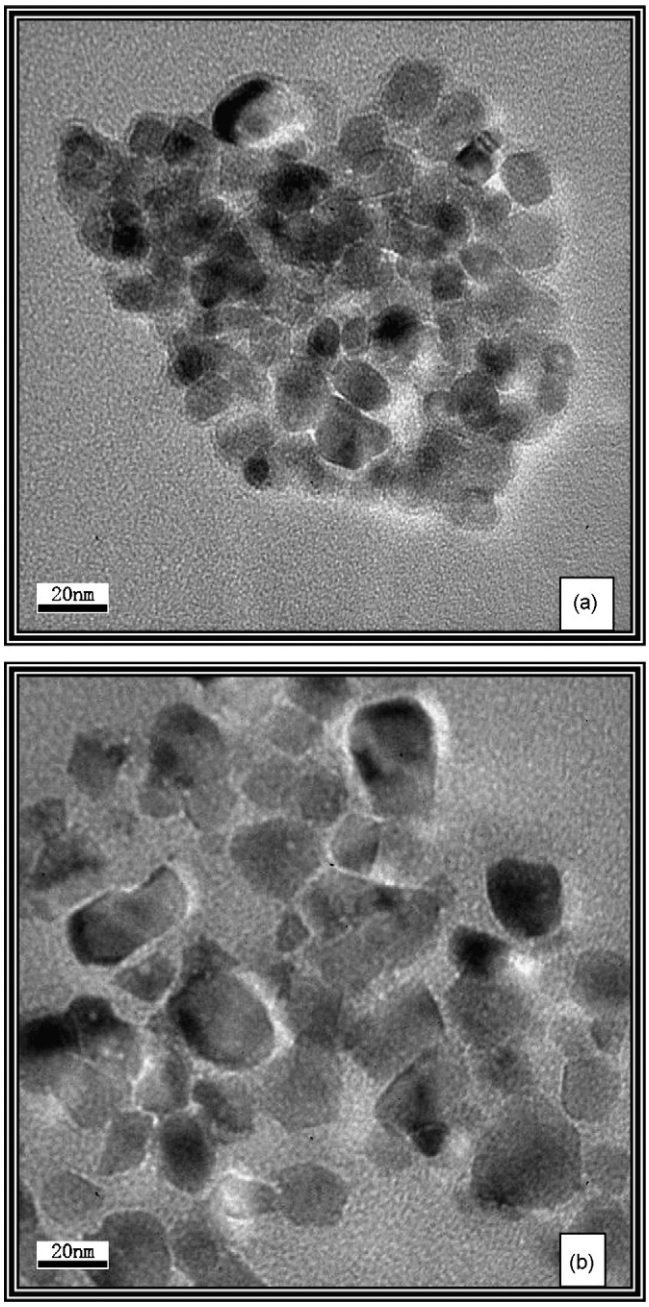

Fig. 3. Transmission electron micrographs of holmium-doped and un-doped TiO_2: (a) TH(0.3)500; (b) T500.

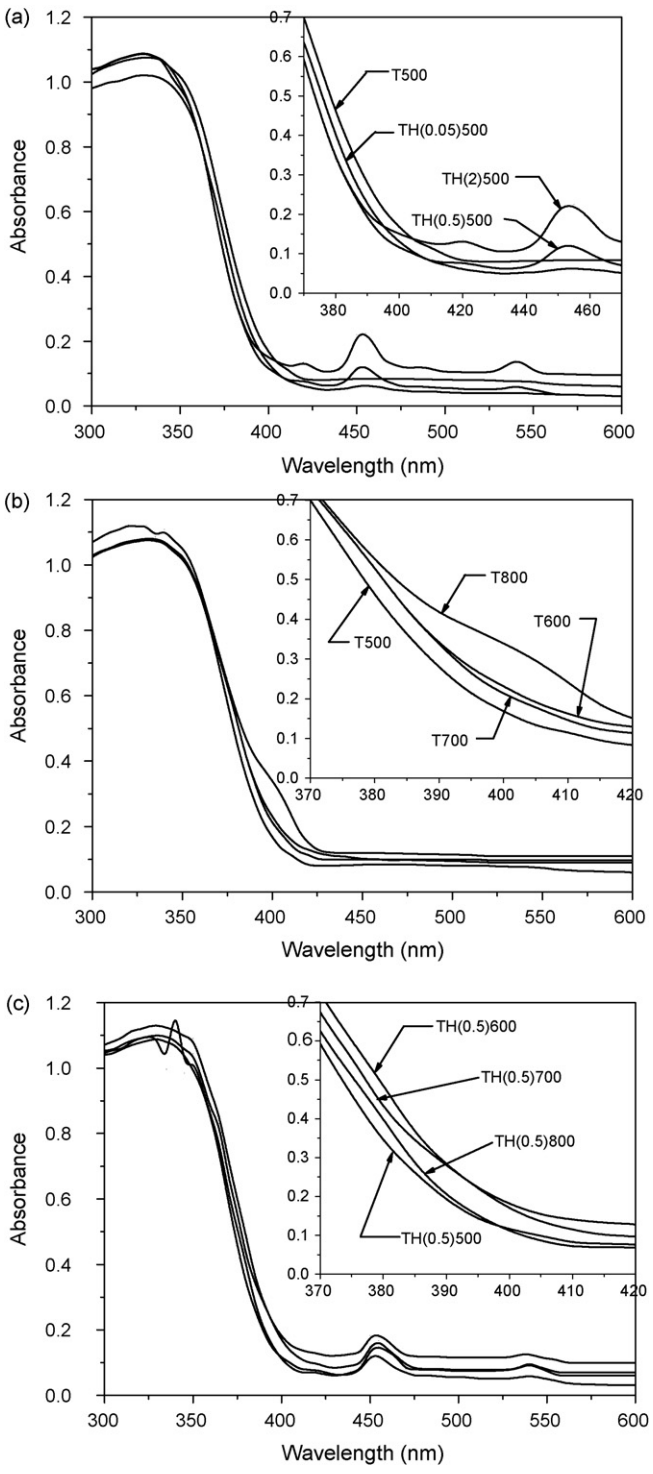

Fig. 4. UV–vis diffuse reflectance spectroscopy of samples.

Samples with larger surface areas could pre-adsorb more methyl orange molecules, which was helpful to avoid the recombination of electron and hole on the surface of catalyst. Smaller crystalline size meant more powerful redox ability due to the quantumsize effect, and smaller crystallite size was in favor of the shifting of photogenerated carriers to the surface of photocatalyst and reacting with reactant. That was, holmium doping might improve the transfer efficiency of photogenerated carriers to surrounding supports and compound adsorbed on photocatalyst matrix. Then, the photocatalytic activity was enhanced. In addition, holmium doping could suppress the recombination of excited electrons and positive holes in the progress of their transferring to the surface of photocatalyst. The substitutions of Ho to Ti ions could create charge imbalance. The charge imbalance should be satiated, so more hydroxide ions would be adsorbed on the surface for charge balance [17]. These hydroxide ions could enhance the separation efficiency of electron–hole pair by trapping holes. Furthermore, hydroxide ions reacted with holes and produced surface hydroxyl radical ($^{\bullet}OH$), which was advantage to improve the photocatalytic degradation of methyl orange. Therefore, the photoinduced charge carriers recombination could be suppressed and the photocatalytic activity of holmium-doped TiO_2 could be promoted.

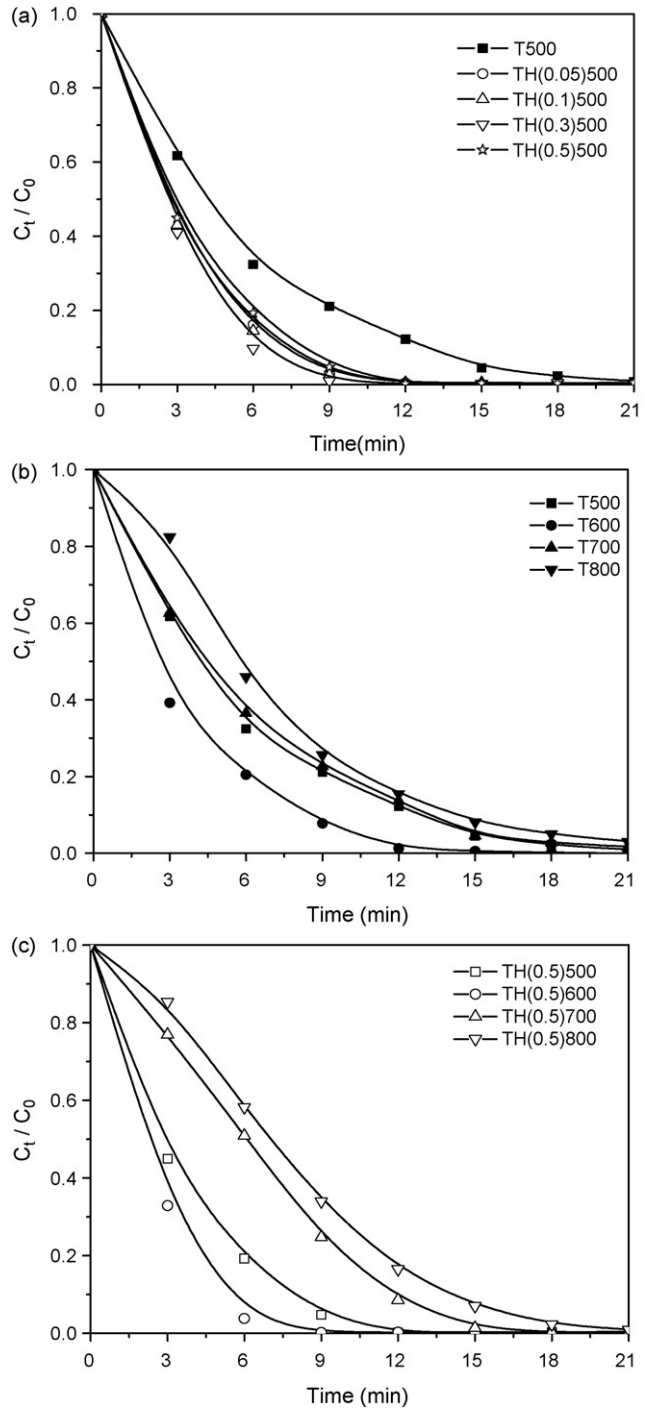

Fig. 5. Degradation curves of methyl orange by samples under mercury lamp irradiation.

The optimum holmium-doped amount was 0.3 mol.% in this investigation, which may be due to the fact that there was an optimum doped content in TiO_2 particles for the most efficient separation of photoinduced electron–hole pairs. The value of the space charge region potential for the efficient separation of electron–hole pairs must be not lower than 0.2 V [31]. As the increase of doped amount, the surface barrier become higher, the space charge region become narrower, and the electron–hole pairs within the region were efficiently separated by the large electric field before recombination. On the other hand, when the concentration of doped ions was high, the space charge region becomes very narrow and the penetration depth of light into TiO_2 exceeded the space charge layer, so the recombination of the photogenerated electron–hole pairs in semiconductor becomes easier. Consequently, there was an optimum concentration of dopant ions to ensure the thickness of space charge layer substantially equal to the light penetration depth [17].

The photocatalytic activity of T800 was the worst among the four un-doped TiO_2 samples, although its absorption profile red-shift extent was the largest. It might due to combine effects of smaller surface area and larger crystallite size. Furthermore, there were 11 wt.% rutiles in sample T800. Anatase has been confirmed to possess higher photocatalytic activity than rutile TiO_2 [32–33]. It could be attributed that the adsorptive affinity of anatase for organic compounds was higher than that of rutile, and anatase phase also exhibited low rate of recombination in comparison to rutile due to its 10-fold greater rate of hole trapping [34].

Fig. 5(b and c) indicated the lower photocatalytic activity of holmium-doped sample calcined at 800 °C than un-doped one calcined at the same temperature. It may be due to the fact that the optimal doped amount was changed with the crystallite size of nanoparticles. Zhang et al. [35] confirmed that the optimal doped amount decreased with crystallite size increase. 0.5 mol.% Ho ions doped in TiO_2 calcined at 800 °C becomes superfluous because of crystallite size increase. Excess amounts of rare earth oxide covering the surface of TiO_2 would increase the number of recombination centers and result in low photoactivity [17].

Comparing with the samples calcined at 500 °C, the samples calcined at 600 °C possessed smaller surface areas and larger crystallite size, which was disadvantage to the photocatalytic activity. But the sample calcined at 600 °C had a more excellent crystallinity, as indicated in Fig. 2. The degree of crystallinity also played a major role in the photoactivity of TiO_2 [18]. The photocatalytic activity of crystallinity TiO_2 was higher than that of uncrystallinity TiO_2, so the optimal calcined temperature was 600 °C finally.

4. Conclusions

Holmium doping decreased crystalline size and increased specific surface area of samples in this investigation. Larger surface areas pre-adsorbed more methyl orange molecules, which were helpful to avoid the recombination of electron and hole on the surface of catalyst, and smaller crystallite size was in favor of the shifting of photogenerated carriers to the surface of photocatalyst and reacting with reactant. Holmium doping led to lattice distortion and expansion of TiO_2, which reduced the recombination rate of electron and hole pairs and produced more hydroxyl radical. Furthermore, holmium doping could create charge imbalance, which suppressed the recombination of excited electrons and positive holes in the catalyst in the progress of their transferring to the surface of photocatalyst. Therefore, holmium doping is an effective means to improve the photocatalytic activity of TiO_2 for degradation organic pollutants in water. In this study, the optimal doped amount was 0.3 mol.% for the maximum photocatalytic degradation ratio when holmium-doped TiO_2 was calcined at 500 °C, and the optimal calcined temperature was 600 °C when the doped amount was 0.5 mol.%. Two absorption peaks around at 450 and 540 nm in holmium-doped TiO_2 may be helpful to improve visible light response of doped TiO_2, which requires further investigation.

References

[1] M. Mohseni, A. David, Gas phase vinyl chloride (VC) oxidation using TiO_2-based photocatalysis, Appl. Catal. B: Environ. 46 (2003) 219–228.
[2] W. Choi, J.Y. Ko, H. Park, J.S. Chung, Investigation on TiO_2-coated optical fibers for gas-phase photocatalytic oxidation of acetone, Appl. Catal. B: Environ. 31 (2001) 209–220.

[3] S. Gelover, P. Mondragón, A. Jiménez, Titanium dioxide sol-gel deposited over glass and its application as a photocatalyst for water decontamination, J. Photochem. Photobiol. A: Chem. 165 (2004) 241–246.
[4] J.M. Herrmann, C. Guillard, J. Disdier, C. Lehaut, S. Malato, J. Blanco, New industrial titania photocatalysts for the solar detoxification of water containing various pollutants, Appl. Catal. B: Environ. 35 (2002) 281–294.
[5] J.C.S. Wu, C.H. Chen, A visible-light response vanadium-doped titania nanocatalyst by sol–gel method, J. Photochem. Photobiol. A: Chem. 163 (2004) 509–515.
[6] H. Yamashita, M. Harada, J. Misaka, M. Takeuchi, K. Ikeue, M. Anpo, Degradation of propanol diluted in water under visible light irradiation using metal ion-implanted titanium dioxide photocatalysts, J. Photochem. Photobiol. A: Chem. 148 (2002) 257–261.
[7] S. Klosek, D. Raftery, Visible light driven V-doped TiO_2 photocatalyst and its photooxidation of ethanol, J. Phys. Chem. B. 105 (2001) 2815–2819.
[8] X.Z. Li, F.B. Li, C.L. Yang, W.K. Ge, Photocatalytic activity of WO_x-TiO_2 under visible light irradiation, J. Photochem. Photobiol. A: Chem. 141 (2001) 209–217.
[9] Y. Yang, X. Li, J. Chen, L. Wang, Effect of doping mode on the photocatalytic activities of Mo/TiO_2, J. Photochem. Photobiol. A: Chem. 163 (2004) 517–522.
[10] M.S. Jeon, W.S. Yoon, H. Joo, T.K. Lee, H. Lee, Preparation and characterization of a nano-sized Mo/Ti mixed photocatalyst, Appl. Surf. Sci. 165 (2000) 209–216.
[11] A. Fuerte, M.D.H. Alonso, A.J. Maira, A.M. Arias, M.F. Garcıa, J.C. Conesa, J. Soria, G. Munuera, Nanosize Ti–W mixed oxides: effect of doping level in the photocatalytic degradation of toluene using sunlight-type excitation, J. Catal. 212 (2002) 1–9.
[12] P. Yang, C. Lu, N. Hua, Y. Du, Titanium dioxide nanoparticles co-doped with Fe^{3+} and Eu^{3+} ions for photocatalysis, Mater. Lett. 57 (2002) 794–801.
[13] L. Jing, X. Sun, B. Xin, B. Wang, W. Cai, H. Fu, The preparation and characterization of La doped TiO_2 nanoparticles and their photocatalytic activity, J. Solid State Chem. 177 (2004) 3375–3382.
[14] Y. Xie, C. Yuan, Characterization and photocatalysis of Eu^{3+}-TiO_2 sol in the hydrosol reaction system, Mater. Res. Bull. 39 (2004) 533–543.
[15] Y. Xie, C. Yuan, Visible-light responsive cerium ion modified titania sol and nanocrystallites for X-3B dye photodegradation, Appl. Catal. B: Environ. 46 (2003) 251–259.
[16] Y. Xie, C. Yuan, X. Li, Mater, photosensitized and photocatalyzed degradation of azo dye using Ln^{n+}-TiO_2 sol in aqueous solution under visible light irradiation, Sci. Eng. B 117 (2005) 325–333.
[17] A.W. Xu, Y. Gao, H.Q. Liu, The preparation, characterization, and their photocatalytic activities of rare-earth-doped TiO_2 nanoparticles, J. Catal. 207 (2002) 151–157.
[18] J. Xiao, T. Peng, R. Lia, Z. Peng, C. Yan, Preparation, phase transformation and photocatalytic activities of cerium-doped mesoporous titania nanoparticles, J. Solid State Chem. 179 (2006) 1161–1170.
[19] A.M. Simas, R.O. Freire, G.B. Rocha, Lanthanide coordination compounds modeling: sparkle/PM3 parameters for dysprosium (III), holmium (III) and erbium (III), J. Organomet. Chem. 693 (2008) 1952–1956.
[20] G.A.H. Mekhemer, Surface acid–base properties of holmium oxide catalyst: in situ infrared spectroscopy, Appl. Catal. 275 (2004) 1–7.
[21] J. Lin, J.C. Yu, An investigation on photocatalytic activities of mixed TiO2-rare earth oxides for the oxidation of acetone in air, J. Photochem. Photobiol. A: Chem. 116 (1998) 63–67.
[22] J. Lin, J.C. Yu, D. Lo, S.K. Lam, Photocatalytic activity of rutile $Ti_{1-x}Sn_xO_2$ solid solutions, J. Catal. 183 (1999) 368–372.
[23] E.L. Crepaldi, G.J. de, A.A. Soler-Illia, D. Grosso, F. Cagnol, F. Ribot, C. Sanchez, Controlled formation of highly organized mesoporous titania thin films: From mesostructured hybrids to mesoporous nanoanatase TiO_2, J. Am. Chem. Soc. 125 (2003) 9770–9786.
[24] T. Tong, J. Zhang, B. Tian, F. Chen, Preparation of Ce-TiO2 catalysts by controlled hydrolysis of titanium alkoxide based on esterification reaction and study on its photocatalytic activity, J. Colloid Interf. Sci. 315 (2007) 382–388.
[25] E. Setiawati, K. Kawano, Stabilization of anatase phase in the rare earth: Eu and Sm ion doped nanoparticle TiO2, J. Alloy Compd. 451 (2008) 293–296.
[26] Z. Xu, Q. Yang, C. Xie, W. Yan, Y. Du, Structure, luminescence properties and photocatalytic activity of europium doped-TiO_2 nanoparticles, J. Mater. Sci. 40 (2005) 1539–1541.
[27] C. Liang, M. Hou, S. Zhou, F. Li, C. Liu, T. Liu, Y. Gao, X. Wang, J. Lu, The effect of erbium on the adsorption and photodegradation of orange I in aqueous Er3+-TiO2 suspension, J. Hazard. Mater. B 138 (2006) 471–478.
[28] N. Venkatachalam, M. Palanichamy, Banumathi Arabindoo, V. Murugesan, Enhanced photocatalytic degradation of 4-chlorophenol by Zr^{4+} doped nano TiO_2, J. Mol., Catal. A: Chem. 266 (2007) 158–165.
[29] M. Saif, M.S.A. Abdel-Mottaleb, Titanium dioxide nanomaterial doped with trivalent lanthanide ions of Tb, Eu and Sm: Preparation, characterization and potential applications, Inorg. Chim. Acta 360 (2007) 2863–2874.
[30] X. Wu, W. Qin, X. Ding, Y. Wen, H. Liu, Z. Jiang, Photocatalytic activity of Eu doped TiO2 ceramic films prepared by microplasma oxidation method, J. Phys. Chem. Solids 68 (2007) 2387–2393.
[31] Y. Wang, H. Cheng, L. Zhang, Y. Hao, J. Ma, B. Xu, W. Li, The preparation, characterization, photoelectrochemical and photocatalytic properties of lanthanide metal-ion-doped TiO_2 nanoparticles, J. Mol. Catal. A: Chem. 151 (2000) 205–216.
[32] J. Zhang, T. Ayusawa, M. Minagawa, K. Kinugawa, H. Yamashita, M. Matsuoka, M. Anpo, Investigations of TiO_2 photocatalysts for the decomposition of NO in the flow system: the role of pretreatment and reaction conditions in the photocatalytic efficiency, J. Catal. 198 (2001) 1–8.
[33] J. Zhu, W. Zheng, B. He, J. Zhang, M. Anpo, Characterization of Fe-TiO_2 photocatalysts synthesized by hydrothermal method and their photocatalytic reactivity for photodegradation of XRG dye diluted in water, J. Mol. Catal. A: Chem. 216 (2004) 35–43.
[34] S. Sakthivel, M.C. Hidalgo, D.W. Bahnemann, S.U. Geissen, V. Murugesan, A. Vogelpohl, A fine route to tune the photocatalytic activity of TiO_2, Appl. Catal. B: Environ. 63 (2005) 31–40.
[35] Z. Zhang, C. Wang, R. Zakaria, Role of particle size in nanocrystalline TiO_2-based photocatalysts, J. Phys. Chem. B 102 (1998) 10871–10878.